Journal Pre-proof

Nonlinear optical response of α-terpinolene and β-phellandrene chromophores: An octupolar gas-to-solvent enhancement able to retain light conduction

Neidy S.S. dos Santos, Sávio Fonseca, André Moura, Antonio R. da Cunha, Patricio F. Provasi, Tarciso Andrade-Filho, Rodrigo Gester

PII: S0030-4026(23)00696-4
DOI: https://doi.org/10.1016/j.ijleo.2023.171199
Reference: IJLEO 171199

To appear in: *Optik - International Journal for Light and Electron Optics*

Received date : 2 March 2023
Revised date : 27 June 2023
Accepted date : 20 July 2023

Please cite this article as: N.S.S. dos Santos, S. Fonseca, A. Moura et al., Nonlinear optical response of α-terpinolene and β-phellandrene chromophores: An octupolar gas-to-solvent enhancement able to retain light conduction, *Optik - International Journal for Light and Electron Optics* (2023), doi: https://doi.org/10.1016/j.ijleo.2023.171199.

This is a PDF file of an article that has undergone enhancements after acceptance, such as the addition of a cover page and metadata, and formatting for readability, but it is not yet the definitive version of record. This version will undergo additional copyediting, typesetting and review before it is published in its final form, but we are providing this version to give early visibility of the article. Please note that, during the production process, errors may be discovered which could affect the content, and all legal disclaimers that apply to the journal pertain.

© 2023 Elsevier GmbH. All rights reserved.

Journal Pre-proof

Nonlinear optical response of α-terpinolene and β-phellandrene chromophores: an octupolar gas-to-solvent enhancement able to retain light conduction

Neidy S.S. dos Santos[a], Sávio Fonseca[a], André Moura[a], Antonio R. da Cunha[b], Patricio F. Provasi[c,d], Tarciso Andrade-Filho[e], Rodrigo Gester[e,f]

[a]*Programa de Pós-Graduação em Química, Universidade Federal do Sul e Sudeste do Pará, Marabá-PA, 68507-590, Brazil.*
[b]*Universidade Federal do Maranhão, UFMA, Campus Balsas, CEP 65800-000, Maranhão, Brazil.*
[c]*Facultad de Ciencias Exactas, Químicas y Naturales, Universidad Nacional de Misiones, Posadas, Argentina.*
[d]*Department of Physics, IMIT, Northeastern University, CONICET, AV. Libertad 5500, W 3404 AAS Corrientes, Argentina.*
[e]*Faculdade de Física, Universidade Federal do Sul e Sudeste do Pará, Marabá-PA, 68507-590, Brazil.*
[f]*Instituto de Física, Universidade de São Paulo, Rua do Matão 1371, São Paulo, SP 05588-090, Brazil.*

Abstract

The search for new materials with improved nonlinear optical (NLO) response is a field of growing interest in materials science. Typically, the dipole $\Phi_{J=1}$ contributions exceed the octupolar $\Phi_{J=3}$ ones and dominate the optical behavior. However, the latter is essential for NLO device engineering. Under this scenario, this work investigates the electronic-optical properties of the α-terpinolene and β-phellandrene molecules within the Hyper-Rayleigh scattering formalism (HRS). It includes solvent contributions using a sequential Monte Carlo / Quantum Mechanics procedure. According to Density Functional Theory analysis, molecular solvatochromism acts differently for the two chromophores. While α-terpinolene undergoes a hypsochromic effect, the β-phellandrene molecule shows moderate bathochromism, both with a strong absorption band in the ultraviolet region ($\lambda_{\max} < 240$ nm), making them attractive for potential UV filters. Regarding the NLO response, both compounds present similar values for the first frequency-dependent hyperpolarizability (β_{HRS}) with values that vary from 62.46 to 138.73 au in aqueous environment, superating urea ($\beta = 42.82$ au), a standard optical material. Furthermore, while one of these chromophores is best described by dipole contributions ($\Phi_{J=1} \approx 68\%$), the other is dominated by the octupolar term ($\Phi_{J=3} \approx 60\%$) even when the solvent moderates it. These characteristics allow the building of optical switches without losing the strength of the NLO response. In addition, the polarization of the solute due to the solvent conveniently reduces the refractive index (n), providing light conduction applications. Therefore, these chromophores can be used to promote a decoupling between dipolar and octupolar contributions in NLO.

Keywords: Nonlinear optics, DFT methods, Solvent effects, Monte Carlo simulations

1. Introduction

Optical materials are a growing group with enormous potential in materials science as they enable a variety of optical devices such as solar cells, field-effect transistors, and light-emitting diodes, which propagate some of the information as fast as the speed of light, in the material, allows. Thus, the decades following the NLO survey were characterized by great efforts to discover and propose new chromophores for a variety of optical applications.

Today it is known that, unlike inorganic compounds, organic chromophores have a particular functionality for optical uses, since they interact better with high-power lasers without breaking down, making it easier to miniaturize the devices built with them and their physicochemical properties can be improved through molecular synthetic techniques. For example, organometallic chromophores have been shown to have lower bandgaps that facilitate electronic transitions, amplifying the magnitude of the first and second hyperpolarizability (β and γ) [1, 2], which are the most relevant NLO parameters.

On the other hand, not only low bandgap materials are interesting. Various initiatives have shown that deep ultraviolet NLO optical materials (absorption edge < 200 nm, bandgap > 6.2 eV) are particularly useful in the fabrication of laser systems, generation of attosecond pulses, construction of semiconductors and uses of photolithography [3]. Also, on the same front, nonmetals, particularly boron-containing chromophores, have shown promise in producing a variety of low refractive index glasses, which is interesting for optical and radiation shielding applications in nuclear medicine and industrial uses [4–7]. Thus, with the expectation of fully exploiting such properties, many efforts have been made to synthesize and correlate the ONL response of these materials to the effects of the environment and mainly the molecular structure of these compounds [8].

However, chemical synthesis is not the only way to control the optical response of a chromophore. Specific solute-solvent interactions, such as the Keeson, London, and Debye forces, affect the electronic structure of the material and influence several, if not all, molecular properties [9]. Molecular solvatochromism, for example, changes in the shape, in-

Email address: gester@unifesspa.edu.br (Rodrigo Gester)

tensity, and position of electronic excitation spectra caused by solvent contributions [9]. Furthermore, there is an intrinsic relationship between the electronic excitations and the NLO response of the material. When the solvent shifts the electronic transition toward higher energies, a hypsochromic shift occurs, while a bathochromic shift denotes a trend toward lower energies [9, 10]. Since the NLO effects are properties that involve the active electrons that are normally delocalized over the whole molecular system, they present an equivalent sensitivity for each part. Thus, one strategy is to choose a solvent that can improve the desired property in specific technological applications.

In an attempt to predict the behavior of NLO, sometimes an experimental discussion can be a difficult task, but molecular modeling techniques associated with appropriate quantum mechanical approximations can be easily applied to give reliable information. Although studies have shown the use of DFT calculations to predict and interpret Hyper-Rayleigh scattering experimental results, they highlight the importance of combining theoretical and experimental approaches to fully understand the NLO properties of materials. Therefore, several papers that discuss how molecular structures can be manipulated to improve an NLO prototype [11–13], or even discuss the effects of quantum mechanics on which is difficult to access experimental techniques [14–16]. The dipolar ($\Phi_{J=1}$) and octupolar ($\Phi_{J=3}$) contributions to β are interesting examples extensively investigated by Zyss *et al.* [17–25].

These contributions are important because they represent different mechanisms of interaction between the material and the external electric field. While the dipole term is associated with the alignment of the electric dipoles in the material, the octupolar contribution, on the other hand, is related to the deformation of the chromophore [26, 27]. When an external electric field is applied, the material deforms, and this deformation leads to an NLO response. In summary, these first hyperpolarizability contributions represent different physical mechanisms by which a material can respond to an external electric field and generate an NLO response. Although most compounds are dominated by a dipolar character [28], octupolar systems are less common but equally relevant as they allow the engineering of NLO devices with specific utilities. Therefore, there is a special concern in the discovery of new octupolar chromophores with high NLO response, or simply in how to tune and decouple these two contributions [22, 24, 29–31].

In the search for new NLO materials, eyes are often focused on so-called natural products, which are molecular systems found in abundance in certain plants and fungi. In this work we present for the first time, the optical behavior of the molecules α-terpinolene and β-phellandrene (see Fig. 1). They are found in *Ferula macrecolea* [32], a bush specie with herbicide action. Both are optically active, the former is the most abundant compound (ca. 77%), and the latter is much lesser abundant (5%).

In an attempt to assess these potentialities, this work uses appropriate quantum chemical methodologies to understand how specific solute-solvent interactions govern the molecular solvatochromism and optical response of these compounds.

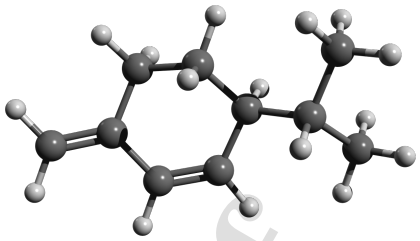

(a) α-terpinilene

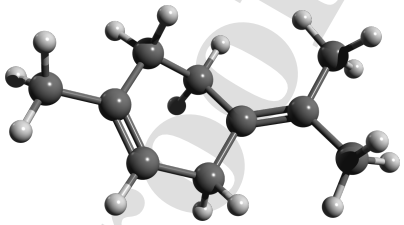

(b) β-phellandrene

Figure 1: The optimized structures of α-terpinolene and β-phellandrene molecules at M062X/6-311++G(*d,p*).

2. Methodology

The analysis of solvent effects, in this work, is based on a sequential Monte Carlo / Quantum Mechanics (s-MC/QM) procedure which applies classical MC simulations to generate uncorrelated liquid structures for further quantum mechanical treatment. The liquid simulations were carried out using the DICE program [34–36] for one solute solvated by 3000 water molecules in the *NpT* ensemble at 1.0 atm and 398 K.

Intermolecular interactions were mediated by the standard Lennard-Jones plus Coulomb potential. While the SPC three-site water potential [37] was used to describe the water molecules, only the LJ parameters of the solute were extracted from the Optimized Parameters for Liquid Simulations [38]. The solute geometry was previously obtained by optimizing the solute molecule in water solvent using the Polarizable-Continuum Model within the Integral Equation Formalism (IEF-PCM) [40]. The Coulomb charges were also obtained using the continuum model with an electrostatic fit of the quantum potential [41].

The simulations were divided into two parts. The first consists of a thermalization stage of 7×10^8 MC steps, followed by a production interval of a further 8×10^9 MC steps in which liquid structures in thermodynamic equilibrium were produced. More details about the simulations and sampling procedure can be found in other works [39].

The contribution of the solvent to the molecular properties of interest has been taken into account using three independent models.

- **Gas-phase**: In this stage, the properties of the isolated molecules of interest are evaluated.
- **PCM**: Designates the Integral-Equation Formalism of the Continuum-Polarizable Model [40] that encloses the solute in a cavity conforming to the shape of the molecule,

and considers the solvent as a continuum environment with a dielectric constant ε.

- **ASEC**: This solvation model designates a single representative normalized configuration of solvent [42] formed by the superposition of one hundred uncorrelated Monte Carlo structures composed of an explicit solute surrounded by 3000 water molecules accounted for only as point charges. This model includes all electrostatic interactions within a radius of 13Å.

- **HB+PC**: This model embeds the solute and the nearest 20 water molecules in the electrostatic field of the remaining 3000 solvent molecules accounted for as point charges. This model couples specific solute-solvent interactions with the electrostatic forces of the bulk molecules.

Regarding the NLO effects, these contributions arise when light interacts with matter. In such a case, the induced molecular dipole moment can be expanded into a Taylor series as:

$$\mu_{\text{ind}}(F) = \mu_i + \sum_j \alpha_{ij}F_j + \frac{1}{2}\sum_{jk}\beta_{ijk}F_jF_k + ... \tag{1}$$

In this equation, μ is the permanent dipole moment, α is the polarizability of the dipole, a tensor of rank 2, whose diagonal components can be combined to give the isotropic contribution (α_{iso})

$$\alpha_{\text{iso}} = \frac{1}{3}(\alpha_{xx} + \alpha_{yy} + \alpha_{zz}). \tag{2}$$

Isotropic polarizability can be used to infer the refractive index (n) using the Lorentz-Lorenz equation [43, 44]

$$\frac{n^2-1}{n^2+2} = \frac{4\pi\alpha_{\text{iso}}}{3V_{\text{mol}}}, \tag{3}$$

where V_{mol} is the molecular volume.

On the other hand, β is a cubic tensor ($3\times3\times3$) with twenty-seven components, and in the presence of frequency-dependent light, this quantity is best described by the hyper-Rayleigh scattering apparatus (β_{HRS}) [46] as

$$\beta_{\text{HRS}}(-2\omega;\omega,\omega) = \beta_{\text{HRS}} = \sqrt{\left\langle\beta^2_{ZZZ}\right\rangle + \left\langle\beta^2_{ZXX}\right\rangle}. \tag{4}$$

In such a formulation,

$$\begin{aligned}\left\langle\beta^2_{ZZZ}\right\rangle = &\frac{1}{7}\sum_i^{x,y,z}\beta^2_{iii} + \frac{1}{35}\sum_{i\neq j}^{x,y,z}\left(\beta^2_{iij} + 4\beta^2_{jii}\right)\\ &+\frac{2}{35}\sum_{i\neq j}^{x,y,z}\left(\beta_{iii}\beta_{ijj} + 4\beta_{jii}\beta_{iij} + 4\beta_{iii}\beta_{jji}\right)\\ &+\frac{1}{105}\sum_{i\neq j\neq k}^{x,y,z}\left(\beta_{iij}\beta_{jkk} + \beta_{iij}\beta_{jkk} + \beta_{ijk}\beta_{jik}\right)\\ &+\frac{4}{105}\sum_{i\neq j\neq k}^{x,y,z}\left(\beta_{jii}\beta_{jkk} + 2\beta^2_{ijk}\right)\end{aligned} \tag{5}$$

and

$$\begin{aligned}\left\langle\beta^2_{ZXX}\right\rangle = &\frac{1}{35}\sum_i^{x,y,z}\beta^2_{iii} + \frac{4}{105}\sum_{i\neq j}^{x,y,z}\left(\beta_{iii}\beta_{ijj} + 2\beta^2_{iij}\right)\\ &+\frac{1}{35}\sum_{i\neq j}^{x,y,z}\left(3\beta^2_{ijj} - 2\beta_{iii}\beta_{jji} - 2\beta_{iij}\beta_{jii}\right)\\ &-\frac{2}{105}\sum_{i\neq j\neq k}^{x,y,z}\left(\beta_{iik}\beta_{jjk} + \beta_{iij}\beta_{jkk} + \beta_{ijk}\beta_{jik}\right)\\ &+\frac{1}{105}\sum_{i\neq j\neq k}^{x,y,z}\left(2\beta^2_{ijk} + \beta_{ijj}\beta_{jkk}\right)\end{aligned} \tag{6}$$

An NLO system can be classified according to its dipolar ($\beta_{J=1}$) and octupolar ($\beta_{J=3}$) terms [21] defined as

$$|\beta_{J=1}|^2 = \frac{3}{5}(\beta_{xxx} + \beta_{xyy})^2, \tag{7}$$

and

$$|\beta_{J=3}|^2 = \frac{1}{20}[3(\beta_{xxx} + \beta_{xyy})^2 + 5(\beta_{xxx} - 3\beta_{xyy})^2]. \tag{8}$$

Throughout the analysis of these components, it is also possible to know how a dipolar or octupolar system can be using the concept of nonlinear molecular anisotropy ratio [19] which is defined from the above equations as follows :

$$\rho = \frac{|\beta_{J=3}|}{|\beta_{J=1}|}. \tag{9}$$

The anisotropic polarizability ciges origen to the dipolar $\Phi_{J=1} = \frac{1}{1+\rho}$ and octupolar $\Phi_{J=3} = \frac{\rho}{1+\rho}$ contributions to β [26]. Furthermore, one has the option of the depolarization ratio (DR), which is defined as [47]

$$\text{DR} = \frac{\left\langle\beta^2_{ZZZ}\right\rangle}{\left\langle\beta^2_{ZXX}\right\rangle}, \tag{10}$$

and also provides information about the dipole and octupolar characteristics of a chromophore.

Finally, the geometries of α-terpinolene and β-phellandrene molecules were optimized at M062X/6-311++G(d,p) (see Fig. 1) while all quantum mechanical calculations were performed considering a variety of DFT-based methods coupled with the 6-311++G(*d,p*) basis set [49, 50] as implemented in the Gaussian 09 program [51]. The analysis of the NLO parameters was performed with Multwfn [52].

3. Results

3.1. Dipole moment and solute polarization

Two chromophores were investigated in this work, α-terpinolene and β-phellandrene, extracted from *Ferula macrecolea* [32]. Table 1 presents the results obtained for the permanent dipole moment (μ) in gas and liquid conditions calculated in the M06-2X/6-311++G(*d,p*) theoretical level.

Journal Pre-proof

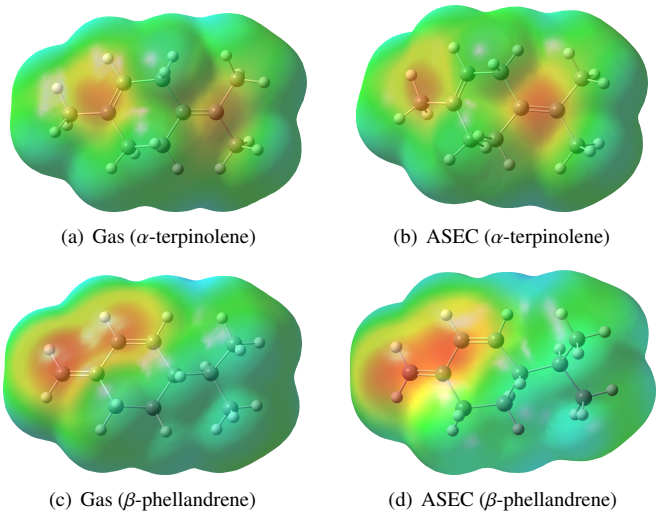

(a) Gas (α-terpinolene) (b) ASEC (α-terpinolene)

(c) Gas (β-phellandrene) (d) ASEC (β-phellandrene)

Figure 2: The molecular electronic potential (MEP) plotted for α-terpinolene (a and b), as well as for β-phellandrene (c and d) in gas and ASEC environments.

The former is the most abundant (ca. 77%) and with the lowest dipolar moment. In the gas phase, the calculation indicates a value of 0.23 D. Whereas in a solvent, within the PCM model, the calculation indicates a value of 0.35 D, which means a polarization effect of 52% with respect to the gas. Within the ASEC model, the calculation indicates an even greater polarization effect, *i.e.* a value of 0.52 D, which is an increase of 126% with respect to the gas.

Fig. 2 plots the molecular electronic potential (MEP) mapping for both molecules, providing an understanding of how the solvent tunes the permanent dipole moment regarding the gas phase. Respectively, deep red and blue colors indicate concentrations of negative and positive electronic densities. From gas to solvent environments, both α-terpinolene and β-phellandrene molecules show an increase of electronic charges on specific molecules sites, while the left side of the molecules becomes bluer. This effect indicates an internal charge transfer procedure mediated by the solvent, which improves μ.

The latter has a much lower abundance (ca. 5%) but with the highest dipolar moment. In the gas phase, the dipolar moment is 0.78 D, but again, the solute polarization is pronounced. The PCM model indicates a value of 1.11 D, which is an increase of 42% with respect to its value in gas, and the ASEC model rise it a bit more giving a value of 1.16 D, which is an increase in the polarization of 49% respect to gas.

The relevance of solute polarization has been reported for several molecular systems. Previous work suggests that larger organic dyes appear to be less sensitive to solvent polarization effects. For example, some azo-dyes indicate a polarization effect that varies between 20% and 30% at the permanent dipole moment [53, 54]. However, small molecules with lower-standing dipole moments are easily polarizable. Some systems such as formamide, uracil, ammonia, and pyridine have undergone shifts between 40

3.2. Dipolar polarizability and refractive index

Table 1 also shows the values obtained for the energy gap (ΔE_{gap}), the isotropic component of the polarizability of the dipole (α_{iso}), the molecular volume (V_{mol}), and the refractive index (n). Concerning the polarizability of the dipole, two aspects must be remarked. First, from α-terpinolene to β-phellandrene there is no significant variation in α_{iso}. For example, in the gas phase, these chromophores show values of 116.56 and 119.24 au, respectively, which means slight contributions from changes in the molecular structure.

The notorious point is the disagreement regarding the prediction of solvent effects on α_{iso}. Therefore, as can be seen in Table 1, the continuous model predicts a value of 154.22 au, which represents an increase of 32.31% with respect to the gas phase, while the discrete model predicts a value of 115.53 au that goes in the opposite direction, showing a net decrease of 0.88% with respect to the gas phase. Likewise, the same results are obtained for β-phellandrene, as can be seen in Table 1.

Since the Lorentz-Lorenz equation allows connecting both α_{iso} and n, the analysis of the refractive index and the electronic structure of the material can indicate what the correct trend would be. Also, Moss's relation, $n^4(\Delta E_{\text{gap}} - 0.365) = 145$ [60], says that the refractive index should vary inversely with the HOMO→LUMO energy gap. Taking the α-terpinolene molecule into account, from gas to solvent, the energy gap increases respectively to 7.48 and 7.85 eV, for PCM and ASEC. Therefore, as determined by the Moss relation, n should be smaller than that reported in gas, but only the ASEC model corresponds to the expectation and predicts a value of 1.48 for the refractive index of α-terpinolene in an aqueous solvent. This rationalization can be extended to β-phellandrene. From gas to solvent, the energy gap increases, consistent for both models, PCM and ASEC, and again only the latter model gives the correct tendency for the refractive index.

As experimental results are not yet appreciable, it is relevant to confirm these predictions using other methods. Table 1 presents results obtained using CAM-B3LYP and ωB97XD, which respectively account for long-range and specific dispersion corrections. As one can realize, these approximations agree very well with M06-2X results.

3.3. UV-Vis spectra interpretation

Figure 3 presents the absorption spectra of the molecules of interest in different environments, and Table 2 shows the main results. For α-terpinolene, the absorption spectrum presents some strong excitations at the limit of the ultraviolet region (190 nm). Although these excitations are readily accessible by computational methods, most spectrometers are blinded to these states. Therefore, we will focus on the region above 190 nm.

The α-terpinolene in the gas phase shows a moderate transition line at 226.43 nm occurring with an oscillator strength of 0.0102 that remarks the lowest-lying spectral region. The analysis of the molecular orbitals indicates a HOMO→LUMO excitation with $n \rightarrow \sigma^*$ symmetry [10].

In most molecules, σ's are the occupied orbitals with the lowest energies, orbitals with π symmetry have slightly higher

Journal Pre-proof

Table 1: The permanent dipole moment (μ/D), the isotropic component of the dipolar polarizability (α_{iso}/au), molecular volume (V_{mol}/Bohr$^3\cdot$ mol^{-1}), and refractive index (n). All parameters were obtained at different DFT/6-31++G* methods:

Chromophore	Method	Medium	μ	α_{iso}	V_{mol}	n	ΔE_{gap}
α-terpinolene	M06-2X	Gas	0.23	116.56	1548.03	1.54	7.38
		PCM	0.35	154.22	1363.74	1.92	7.48
		ASEC	0.52	115.53	1676.83	1.48	7.85
	CAM-B3LYP	Gas	0.24	116.45	1584.89	1.53	7.91
		PCM	0.36	153.71	1326.88	1.75	8.00
		ASEC	0.52	115.34	1354.37	1.63	8.35
	ωB97XD	Gas	0.24	116.51	1234.74	1.72	9.19
		PCM	0.37	154.27	1290.03	2.00	9.29
		ASEC	0.53	115.51	1418.86	1.60	9.44
β-phellandrene		Gas	0.78	119.24	1502.38	1.57	7.40
		PCM	1.11	159.61	1555.41	1.80	7.57
		ASEC	1.16	118.52	1504.77	1.57	7.65
	CAM-B3LYP	Gas	0.83	119.48	1272.61	1.72	7.93
		PCM	1.19	159.72	1502.39	1.85	8.01
		ASEC	1.21	118.67	1430.47	1.61	8.06
	ωB97XD	Gas	0.84	119.58	1343.31	1.67	9.18
		PCM	1.20	160.38	1555.41	1.81	9.20
		ASEC	1.23	118.85	1465.32	1.59	9.23

Table 2: The lowest-lying electronic absorption of α-terpinolene and β-phellandrene in different environments. All parameters were obtained at the M06-2X/6-311++G(d,p) level of calculation:

Chromophore	Medium	λ	Osc. Force	$\Delta\lambda = \lambda_{sol} - \lambda_{gas}$
α-terpinolene	Gas	226.43	0.0102	
	PCM	224.13	0.0124	−2.30
	ASEC	213.11	0.0147	−13.32
	HB+PC	218.20 ± 1.24	0.028 ± 0.003	−8.23 ± 1.24
β-phellandrene	Gas	224.91	0.5114	
	PCM	229.66	0.6803	4.75
	ASEC	222.60	0.6039	−2.31
	HB+PC	233.82 ± 0.62	0.359 ± 0.019	8.91 ± 0.62

energy levels, and the lone pair states or nonbinding orbitals (n) populate even higher energies. Concerning the unoccupied orbitals, the anti-bonding states (π^* and σ^*) are those with the highest energies. For these reasons, it is expected that $n \rightarrow \pi^*$ and $\pi \rightarrow \pi^*$ transitions occur before the $n \rightarrow \sigma^*$ ones, as in α-terpinolene.

Then, for the PCM and ASEC models, the solvent imposes a hypsochromic effect on the $n \rightarrow \sigma^*$ excitation. For example, according to PCM, the solvent shifts the excitation to 224.30 nm, which means a slight blueshift of −2.30 nm from the gas phase spectrum. The second model, ASEC, confirms molecular hypsochromism and sketches that the state should occur at −213.11 nm with a strong oscillator force of 0.0147. Thus, the result indicates a shift of −13.32 nm toward higher energies.

In contrast to the purely electrostatic descriptions, the HB+PC model allows an extension of the wave function methods to the closest solvent molecules, considering the long-range electrostatic effects of the bulk molecules. Of course, this model is the most consistent once it considers specific solute-solvent interactions like the Keeson, London, and Dedye forces.

Figure 5 depicts a typical hydration shell around the solute molecule sampled from the classical MC simulations. Since the α-terpinolene molecule is an aprotic and low polar chromophore, the water molecules of solvents better form hydrogen bonds with each other. This fact means that dipole-dipole and dipole-induced forces play a relevant role in the liquid coordination around the solute that impacts the electronic structure of the chromophores. The HB+PC estimation indicates that the $n \rightarrow \sigma^*$ absorption should occur at 218.20 ± 1.24 nm, meaning a hypsochromic displacement of −8.23 ± 1.24 nm. Furthermore, the solvent not only affects the relative position of the spectral lines $\pi \rightarrow \pi^*$, but according to the forces of the oscillator, the solvent also makes such excitation more intense. One can easily compare these two effects by analyzing Fig. 3.

For β-phellandrene, the effect of the solvent is quite different, see also Figure 5. In gas, there is a very strong HOMO→LUMO+1 excitation at 224.91 nm, that occurs with an oscillator force of 0.5114. After a quick analysis of these orbitals in Fig. 6, it is noted that both orbitals involved in the jump are $\pi \rightarrow \pi^*$.

For such type of excitation, it is expected that a polar solvent like water shifts $\pi \rightarrow \pi^*$ lines to higher wavelengths, which means that the energy of the transition decreases in the solvent (bathochromic) [10]. However, a hypsochromic effect is observed, which in principle is not prohibited for the transition $\pi \rightarrow \pi^*$ but generally, they occur only under specific conditions [61, 62].

Table 2 shows that the PCM and the ASEC calculations go in opposite directions with respect to the gas phase. For instance, while PCM corroborates the expectative and predicts a bathochromic shift of 4.75 nm, the ASEC estimation indicates a blue shift of −2.31 nm. The HB+PC model support that the bathochromism is the right behavior for this $\pi \rightarrow \pi^*$ in β-

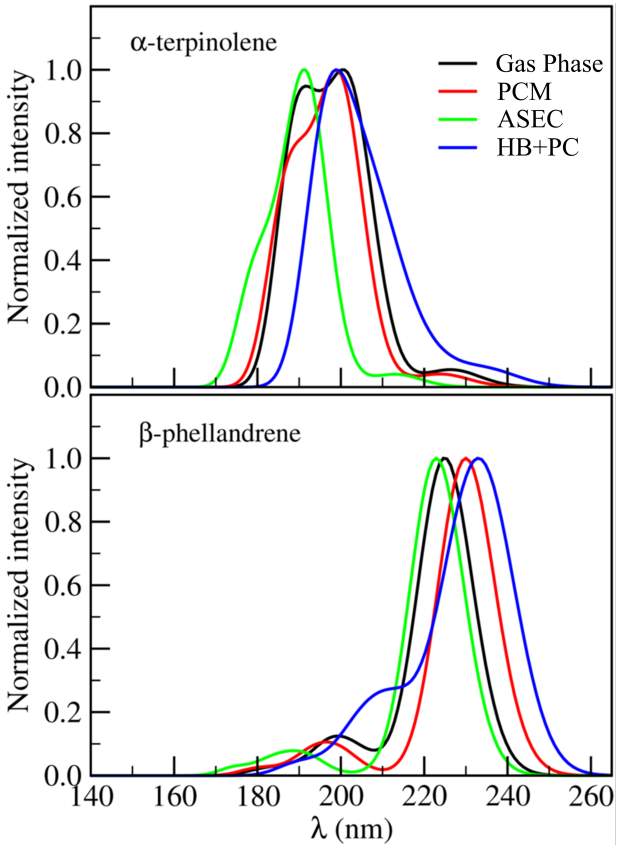

Figure 3: The electronic absorption spectra of α-terpinolene (top) and β-phellandrene (bottom) within different environment models.

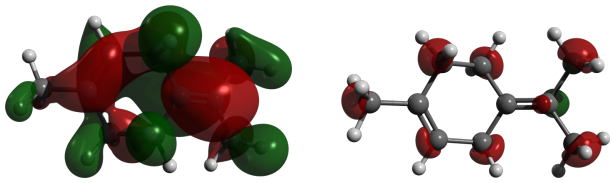

(a) n (HOMO) (b) σ^* (LUMO)

Figure 4: The molecular orbitals involved in the lowest-lying $n \rightarrow \sigma^*$ electronic excitation of α-terpinolene in the gas phase.

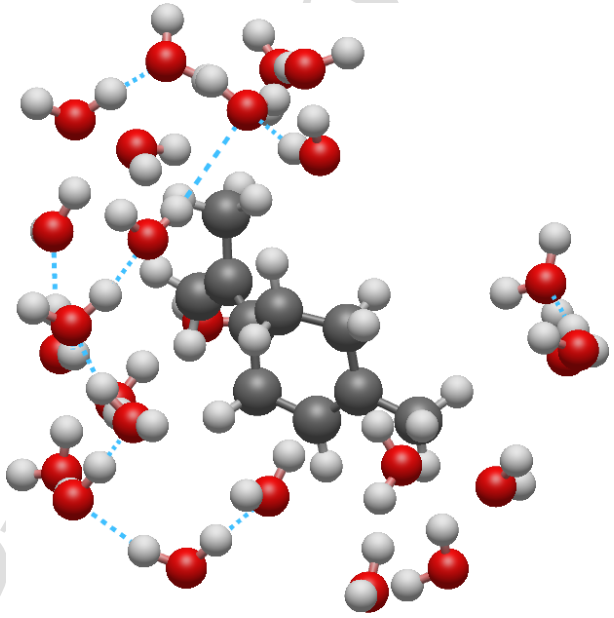

(a) α-terpinolene

Figure 5: A typical hydration shell sampled to form the classical Monte Carlo simulations. The dashed lines represent hydrogen-bond interactions formed between the solvent molecules. The solute is hydrophobic, therefore there are no such solute-solvent structures.

phellandrene. Consistently with this estimation, the maximum absorption should occur around 233.82 ± 0.62 nm, which represents a redshift of 8.91 ± 0.62 nm, as best seen in Fig. 3. Moreover, for one configuration sampled from the MC simulations, Fig. 6 shows the molecular orbitals responsible for such transition in the presence of the solvent. As one can see, these eigenstates are localized on the solute molecule, which means no charge transfer to the solvent.

3.4. First hyperpolarizability

Table 3 presents the frequency-dependent data collected for the first hyperpolarizability within the Hyper-Rayleigh scattering (HRS) formalism. In gas-phase, both chromophores show similar results, 66.18 and 63.46 au respectively, for the α-terpinolene a β-phellandrene molecules.

According to Oudar and Chemla's relation [63], the first hyperpolarizability should vary inversely with the energy gap as ($\beta \propto 1/\Delta E_{\text{gap}}^3$) when accounting for the gas-to-solvent effect. For β-phellandrene, the predictions made with the PCM and ASEC models follow Oudar and Chemla's prevision. Where the energy gap increases by 0.17 and 0.25 eV respectively, which renders an increase of β_{HRS} to 105.86 au as reported by PCM, and to 80.79 au as reported by ASEC.

For α-terpinolene, on the contrary, the solvent also increases the energy gap making the system more insulating. The ASEC model, for instance, predicts an increase of 0.47 eV from gas to solvent, which downs β_{HRS} to 62.6 au. whereas, the PCM model shows the opposite trend for the first hyperpolarizability.

Furthermore, the results suggest that the NLO behavior of α-terpinolene is less sensitive to environmental effects than β-phellandrene. According to the ASEC model, from gas to solvent, β_{HRS} shows a variation of only 5.62% for α-terpinolene, while the variation is 26.25% for β-phellandrene.

Again, due to the absence of experimental results, we confront the M06-2X data to those obtained using CAM-B3LYP and ωB97XD methods (see Table 3). One more time, despite different philosophies, these methods agree very well and confirm the results.

Compared to other standard NLO materials, both α-terpinolene, and β-phellandrene exhibit good performance. For example, Alam [66] and Abbas [67] reported 42.82 au for the first hyperpolarizability of urea in the gas phase, which is far from the current results reported for the studied chromophores in this work. Furthermore, the NLO properties are additive pa-

Table 3: The first hyperpolarizability (β_{HRS}/au), the dipolar ($\Phi_{J=1}$) and octupolar ($\Phi_{J=3}$) contributions, anisotropic polarizability (ρ), depolarization ratio (DR), and energy gap (ΔE_{gap}/eV). All parameters were obtained at different DFT/6-31++G* models quantum mechanics:

Chromophore	Method	Medium	β_{HRS}	$\lvert\beta_{J=1}\rvert$	$\lvert\beta_{J=3}\rvert$	$\Phi_{J=1}$	$\Phi_{J=3}$	ρ	DR	ΔE_{gap}
α-terpinolene	M06-2X	Gas	66.18	101.252	148.533	0.405	0.595	1.467	3.10	7.38
		PCM	85.96	132.529	191.298	0.409	0.591	1.443	3.14	7.48
		ASEC	62.46	97.348	137.294	0.415	0.585	1.410	3.20	7.85
	CAM-B3LYP	Gas	66.87	103.153	148.716	0.410	0.590	1.442	3.14	7.91
		PCM	87.69	137.623	191.190	0.419	0.582	1.389	3.24	8.00
		ASEC	62.67	98.284	136.731	0.418	0.582	1.391	3.24	8.35
	ωB97XD	Gas	65.14	91.296	158.450	0.366	0.634	1.736	2.72	9.19
		PCM	86.86	124.873	206.981	0.376	0.624	1.658	2.81	9.29
		ASEC	62.88	90.692	149.420	0.378	0.622	1.648	2.83	9.44
β-phellandrene	M06-2X	Gas	63.92	125.648	77.858	0.617	0.383	0.620	6.02	7.40
		PCM	105.86	210.064	121.223	0.634	0.366	0.577	6.27	7.57
		ASEC	80.79	163.939	76.299	0.682	0.318	0.465	6.97	7.65
	CAM-B3LYP	Gas	84.31	170.231	83.735	0.670	0.330	0.492	6.80	7.93
		PCM	132.72	269.143	126.175	0.681	0.319	0.469	6.95	8.01
		ASEC	97.73	199.884	84.017	0.704	0.296	0.420	7.26	8.06
	ωB97XD	Gas	87.43	176.50	86.964	0.670	0.330	0.493	6.80	9.18
		PCM	138.73	281.016	133.498	0.678	0.322	0.475	6.91	9.20
		ASEC	100.78	206.404	85.096	0.708	0.292	0.412	7.31	9.23

rameters, which means that it is possible to build devices with improved NLO behavior by packing or crystallizing a chromophore [68]. These features open up possibilities for the use of α-terpinolene and β-phellandrene.

3.5. Dipolar $\Phi_{J=1}$ and octupolar $\Phi_{J=3}$ contributions

The NLO response of a chromophore can be divided into dipolar and octupolar contributions as $\Phi_{J=1} + \Phi_{J=3}$. After analyzing the results shown in Table 3, two effects are observed. First, the structural impacts. For instance, from α-terpinolene to β-phellandrene, there is an inversion of the contributions, $\Phi_{J=1}$ and $\Phi_{J=3}$, in the gas phase. The octupolar contribution predominates ($\Phi_{J=3}$ = 59.5%) for β-phellandrene, whereas the β-phellandrene molecule is ruled by the dipolar contribution with $\Phi_{J=1}$ = 61.7%.

The character of the contribution to the NLO response of a chromophore can best be analyzed using the anisotropy ratio (ρ), for which, when $\rho \to 0$, the system is purely dipolar. Otherwise, when $\rho \to \infty$, the chromophore is said to be predominantly octupolar. From Table 3, it can be seen that the anisotropy ratio for α-terpinolene (ρ = 1.467) is more than double that obtained with β-phellandrene (ρ = 0.620) in gas, confirming that the first compound is much more octupolar than the second.

The second aspect that must be accounted for is the solvent effect. For a ground state system, the polarization due to solvent normally acts improving the dipole moment. Thus, the default is that the solvent enhances the dipolar contribution at the expense of the octupolar term. Table 3, it is verified that this statement is verified in an accentuated form for the β-phellandrene molecule. Thus, the PCM and ASEC models predict respectively dipolar contributions of 63.4 and 68.2%, which exceed the prognosis in gas ($\Phi_{J=1}$ = 61.7%).

However, the mentioned effect is slighter for α-terpinolene. Consistent with the quantum mechanical prediction, the solvent hardly affects the different contributions to the first hyperpolarizability. For example, the PCM and ASEC models indicate $\beta^{J=3}$ contributions of 59.1 and 58.5%, respectively, which are very close to those reported for α-terpinolene in gas, 59.5%

The depolarization ratio (DR) also exposes the dipolar and octupolar characters of the chromophores by analyzing the averages $\langle\beta^2_{ZZZ}\rangle$ and $\langle\beta^2_{ZXX}\rangle$. Within the DR scale, the extremes lie between the octupolar (1.5) and dipole (9) characters. According to Table 3, for example, in gas, the depolarization ratio ranges from 3.10 for α-terpinolene to 6.02 for β-phellandrene, indicating that the first chromophore is the most octupolar.

Thus, since these two chromophores have similar values for β_{HRS}, one can use them for constructing gates that alternate be-

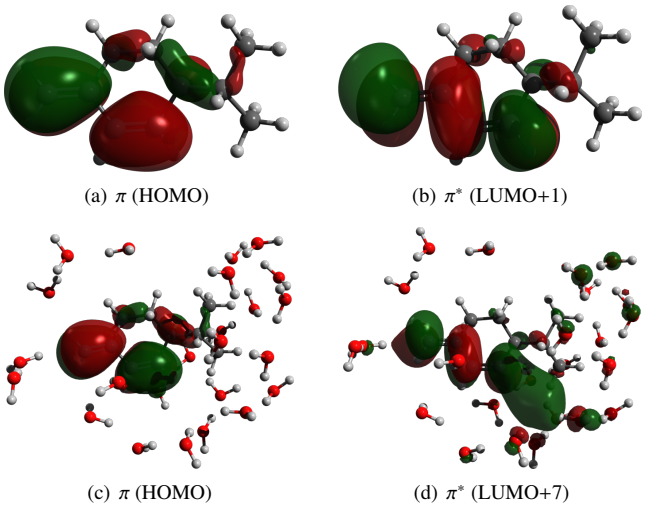

(a) π (HOMO) (b) π^* (LUMO+1)

(c) π (HOMO) (d) π^* (LUMO+7)

Figure 6: The molecular orbitals involved in the lowest-lying $\pi \rightarrow \pi^*$ electronic excitation of β-phellandrene in the gas phase (a and b), as well as in the presence of the explicit water molecules (c and d).

tween dipolar and octupolar responses without losing the intensity of the NLO response.

4. Conclusions

This work presents a theoretical discussion about the solvent effect on the NLO response of α-terpinolene and β-phellandrene, two chromophores originally extracted from *Ferula macrecolea*. The investigation is based on a sequential MC/DFT procedure and takes advantage of both solvation models, continuum and discrete, and of the frequency-dependent Hyper-Rayleigh scattering formalism to discuss the optical behavior of such compounds.

The results indicate that the solvent affects all relevant electrical properties. Hence, within the ASEC model, there is an increase for the gas-to-solvent effect of 126% concerning the gas phase for α-terpinolene and from 42 to 49% for β-phellandrene. The refractive indices are lower than their counterparts in the gas phase. This means that the environment improves their ability to conduct light and therefore, information and points toward a potential use in optoelectronics and telecommunications.

The UV-visible spectra, gas-to-solvent, show a shift toward higher energies as much as -13.32 nm for α-terpinolene within the ASEC model and mixed trend for β-phellandrene (Table 2), but more likely a shift to lower energies according to the best model, HB-PC.

In addition to these discoveries, the first frequency-dependent hyperpolarizability (β_{HRS}), which is the main NLO parameter, shows, in the solvent, values comparable to those reported for urea, a standard optical compound. Regarding the dipolar and octupolar contributions to the first hyperpolarizability, β-phellandrene, and α-terpinolene present different behaviors. While the dipole prescriptions better describe the former compound, the latter is a non-trivial system, whose octupolar contribution drives its optical response. Since both chromophores have a similar NLO intensity, it is possible to switch between dipole and octupolar circuits without losing optical response. These findings for n and β_{HRS} suggest that both α-terpinolene and manly β-phellandrene may hold promise for optical applications.

Acknowledgments

This study is financed in part by the Coordenação de Aperfeiçoamento de Pessoal de Nível Superior - Brasil (CAPES), Conselho Nacional de Desenvolvimento Científico e Tecnologico (CNPq), and Fundação de Amazônica de Amparo a Estudos e Pesquisas (FAPESPA). P.F.P. acknowledges financial support from CONICET (PIP: KE3-11220200100467CO).

References

[1] H.S. Nalwa, Organometallic materials for nonlinear optics, *Applied Organometallic Chemistry*, **5** (1991) 349. DOI: 10.1002/aoc.590050502

[2] S. Taboukhat, N. Kichou, J.-L. Fillaut, O. Alévêque, K. Waszkowska, A. Zawadzka, A. El-Ghayoury, A. Migalska-Zalas, B. Sahraoui, Transition metals induce control of enhanced NLO properties of functionalized organometallic complexes under laser modulations, *Sci. Rep.* **10** (2020) 15292. DOI: 10.1038/s41598-020-71769-2.

[3] T. T.Tran, H. Yu, J. M. Rondinelli, K. R. Poeppelmeier, P. S. Halasyamani, Deep Ultraviolet Nonlinear Optical Materials, *Chem. Mater.* **28** (2016) 5238. DOI: 10.1021/acs.chemmater.6b02366.

[4] Z. A. Alrowaili, A. M. Ali, A.M. Al-Baradi, M. S. Al-Buriahi, E. A. A. Wahab, Kh. S. Shaaban, A signifcant role of MoO3 on the optical, thermal, and radiation shielding characteristics of B2O3–P2O5–Li2O glasses, *Optical and Quantum Electronics* **54** (2022) 88. DOI: 10.1007/s11082-021-03447-0.

[5] M. S. Al-Buriahi, M. Hessien, F. Alresheedi, A. M. Al-Baradi, Z.A. Alrowaili, I. Kebaili, I. O. Olarinoye, ZnO-Bi2O3 nanopowders: Fabrication, structural, optical, and radiation shielding properties, *Ceramics International*, **48** (2022) 3464. DOI: 10.1016/j.ceramint.2021.10.124.

[6] Z.A. Alrowaili, T.A. Taha, M. Ibrahim, K.M.A. Saron, C. Sriwunkum. A.M. Al-Baradi, M.S. Al-Buriahi, Synthesis and characterization of B2O3-Ag3PO4-ZnO-Na2O glasses for optical and radiation shielding applications, *Optik - International Journal for Light and Electron Optics* **248** (2021) 168199. DOI: 10.1016/j.ijleo.2021.168199.

[7] J.S. Alzahrani, A. Sharma, S.N. Nazrin, Z.A. Alrowaili, M.S. Al-Buriahi, Optical and radiation shielding effectiveness of a newly fabricated WO3 doped TeO2–B2O3 glass system, *Radiation Physics and Chemistry* **193** (2022) 109968. DOI: 10.1016/j.radphyschem.2022.109968.

[8] M. Mutailipu, K.R. Poeppelmeier, K.R. Poeppelmeier, Borates: A Rich Source for Optical Materials, *Chem. Rev.* **121** (2021) 1130. DOI: 10.1021/acs.chemrev.0c00796.

[9] Christian Reichardt, Thomas Welton, Solvents and Solvent Effects in Organic Chemistry, Wiley-VCH Verlag GmbH & Co. KGaA, 2010, DOI: 10.1002/9783527632220.

[10] D.L. Pavia, G.M. Lampman, G.S. Kriz, J.R. Vyvyan, Introduction to Spectroscopy, International, 4th edition, Cengage Learning, 2008, pp.381-817.

[11] M. Khalid, S. Naseer, M.S. Tahir, I. shafiq, K.S. Munawar, S.F.A. Morais, A.A.C. Braga, A theoretical approach towards designing of banana shaped non-fullerene chromophores using efficient acceptors moieties: exploration of their NLO response properties, *Optical and Quantum Electronics* **55** (2023) 258. DOI: 10.1007/s11082-022-04441-w.

[12] S.R. Marder, B. Kippelen, A.C.-Y. Jen, N. Peyghambarian, Design and synthesis of chromophores and polymers for electro-optic and photorefractive applications, *Nature*, **388** (1997) 845. DOI: 10.1038/42190.

[13] P. Wang, P. Zhu, W. Wu, H. Kang, C. Ye. Design of novel nonlinear optical chromophores with multiple substitution, *Phys. Chem. Chem. Phys.*, **1** (1999) 3519. DOI: 10.1039/A903535D.

[14] A. Raiol, A.R. da Cunha, V. Manzoni, T. Andrade-Filho, R. Gester Solvent enhancement and isomeric effects on the NLO properties of a photoinduced cis-trans azomethine chromophore: A sequential MC/QM study Author links open overlay panel, *Journal of Molecular Liquids*, **340** (2021) 116887. DOI: 10.1016/j.molliq.2021.116887.

[15] R.Gester, A. Torres, A.R. da Cunha, T. Andrade-Filho, V. Manzoni, Theoretical study of thieno[3,4-b]pyrazine derivatives with enhanced NLO response, *Chemical Physics Letters*, **781** (2021) 138976. DOI: 10.1016/j.cplett.2021.138976.

[16] R. Gester, A. Torres, C. Bistafa, R.S. Araújo, T.A. da Silva, V. Manzoni Theoretical study of a recently synthesized azo dyes useful for OLEDs, Materials Letters, *Materials Letters*, **280** (2020) 128535. DOI: 10.1016/j.matlet.2020.128535.

[17] J. Zyss, G. Berthier, *J. Chem. Phys.* **1982**, 77, 3635.

[18] M. Joffre, D. Varon, R.J. Silbey, J. Zyss, *J. Chern. Phys.* **1992**, 97, 5607-5615.

[19] J. Zyss, Molecular engineering implications of rotational invariance in quadratic nonlinear optics: From dipolar to octupolar molecules and materials, J. Chem. Phys. 98, 6583 (1993). DOI: 10.1063/1.464802.

[20] J. Zyss, S. Brasselet, *J. Nonlinear Opt. Phys. Mater.* **1998**, 7, 397.439.

[21] J. Zyss, S. Brasselet, Multipolar Symmetry Patterns in Molecular Nonlinear Optics, Journal of Nonlinear Optical Physics & Materials, 07, 397-439 (1998) DOI: 10.1142/S0218863598000302.

[22] Katell Sénéchal, Olivier Maury, Hubert Le Bozec, Isabelle Ledoux, Joseph Zyss, Zinc(II) as a Versatile Template for the Design of Dipolar and Octupolar NLO-phores, J. Am. Chem. Soc. 2002, 124, 17, 4560–4561. DOI: 10.1021/ja025705a.

[23] M. Cho, S.Y. An, H. Lee, I. Ledoux, J. Zyss, *J. Chem. Phys.* **2002**, 116, 9165-9173.

[24] Christian G. Claessens, David González-Rodríguez, Tomás Torres, Guillermo Martín, Fernando Agulló-Lóez, Isabelle Ledoux, Joseph Zyss, Victor R. Ferro, José M. García de la Vega, Structural Modulation of the Dipolar-Octupolar Contributions to the NLO Response in Subphthalocyanines, J. Phys. Chem. B, 2005, 109, 9, 3800-3806, DOI: 10.1021/jp045322u.

[25] S. Bidault, S. Brasselet, J. Zyss, *J. Chem. Phys.* **2007**, 126, 034312.

[26] L. Zhang, D. Qi, L. Zhao, C. Chen, Y. Bian, W. Li, Density functional theory study on subtriazaporphyrin derivatives: dipolar/octupolar contribution to the second-order nonlinear optical activity, J. Phys. Chem. A **116** (2012) 10249. DOI: 10.1021/jp3079293.

[27] S. Fonseca, N.S.S. dos Santos, A.R. da Cunha, S. Canuto, P.F. Provasi, T. Andrade-Filho, R. Gester, The Solute Polarization and Structural Effects on the Nonlinear Optical Response of Based Chromone Molecules, *ChemPhysChem* (2023) DOI: 10.1002/cphc.202300060.

[28] David R. Kanis, Mark A. Ratner, J. Tobin, Marks. Design and construction of molecular assemblies with large second-order optical nonlinearities. quantum chemical aspects, *Chem. Rev.* **94** (1994) 195-242. DOI: 10.1021/cr00025a007.

[29] Cui-Cui Yang, Xue-Lian Zheng, Jiu Chen, Wei Quan Tian, Wei-Qi Li, Ling Yang, Spin engineering of triangulenes and application for nano nonlinear optical materials design, Phys. Chem. Chem. Phys., 2022, 24, 18529-18542. DOI: 10.1039/D2CP02915D.

[30] Linh Tran Bao Nguyen, Cheng-Lin Wu, Tzu-Chau Lin, Manabu Abe, Tris(4'-Nitrobiphenyl)amine-An Octupolar Chromophore with High Two-Photon Absorption Cross-Section and Its Application for Uncaging of Calcium Ions in the Near-Infrared Region, J. Org. Chem. 2022, 87, 23, 15888–15898. DOI: 10.1021/acs.joc.2c01987.

[31] Olivier Maury, Hubert Le Bozec, Molecular Engineering of Octupolar NLO Molecules and Materials Based on Bipyridyl Metal Complexes, Accounts of Chemical Research 2005, 38, 9, 691-704. DOI: 10.1021/ar020264l.

[32] H. Abdelkader, Z. Farouk, M. Mohamed, M, Abdelghani, L. Houdheifa, K. Imene, H. Ines, B. Anis, C. Nadji, H. Meriem, R. Souada, T. Lasnouni, L.B. Omar, Efficient one-pot synthesis, characterization and Â DFT study of solvents polarity effects on the structural, energetic and thermodynamic proprieties of (a-methylamino-ethyl)-phosphonic acid dimethyl ester, *Journal of Molecular Structure*, textbf1272, 134165 (2023). DOI: 10.1016/j.molstruc.2022.134165.

[33] P. V. Artyushenko, F. N. Tomilin, A. A. Kuzubovb , S. G. Ovchinnikov, P. E. Tsikalova , T. M. Ovchinnikova, V. G. Soukhovolsky, The Stability of the Pheromones of Xylophagous Insects to Environmental Factors: An Evaluation by Quantum Chemical Analysis, Biophysics, 2017, Vol. 62, No. 4, pp. 532–538.DOI: 10.1134/S0006350917040029.

[34] H.M. Cezar, S. Canuto K. Coutinho, DICE: A Monte Carlo program for molecular liquid simulation, University of São Paulo, São Paulo, v. 3.0, University of São Paulo, São Paulo, v. 3.0, 2018.

[35] H.M. Cezar, S. Canuto, Kaline Coutinho, Solvent effect on the syn/anticonformational stability: A comparison between conformational bias Monte Carlo and molecular dynamics methods, *International Journal of Quantum Chemistry*, **119**, e25688 (2018). DOI: 10.1002/qua.25688.

[36] H.M. Cezar, Sylvio Canuto, Kaline Coutinho, DICE: A Monte Carlo Code for Molecular Simulation Including the Configurational Bias Monte Carlo Method, *Journal of Chemical Information and Modeling*, *60*, 3472 (2020). DOI: 10.1021/acs.jcim.0c00077.

[37] H.J.C. Berendsen, J.P.M. Postma, W.F. van Gunsteren, and J. Hermans, In Intermolecular Forces, edited by B. Pullman (Reidel, Dordrecht, 1981), p. 331.

[38] J. Pranata, S.G. Wierschke, W. Jorgensen, OPLS potential functions for nucleotide bases. Relative association constants of hydrogen-bonded base pairs in chloroform, *Journal of the American Chemical Society*, **113**, 2810 (1991). DOI: 10.1021/ja00008a002.

[39] S.C.S. Costa, R.M. Gester, J.R. Guimarães, J.G. Amazonas, J. Del Nero, S.B.C. Silva, A. Galembeck, The entrapment of organic dyes into sol–gel matrix: Experimental results and modeling for photonic applications, *Opt. Matt.* **30**, 1432 (2008). DOI: 10.1016/j.optmat.2007.08.008.

[40] S. Miertuš, E. Scrocco, and J. Tomasi, Electrostatic Interaction of a Solute with a Continuum. A Direct Utilization of ab initio Molecular Potentials for the Prevision of Solvent Effects, *Chem. Phys.*, **55**, 117 (1981). DOI: 10.1016/0301-0104(81)85090-2.

[41] C.M. Breneman, K.B. Wiberg, Determining atom-centered monopoles from molecular electrostatic potentials – the need for high sampling density in formamide conformational-analysis, *J. Comp. Chem.*, **11**, 361 (1990). DOI: 10.1002/jcc.540110311.

[42] K. Coutinho, H.C. Georg and T.L. Fonseca, V. Ludwig, S. Canuto, An efficient statistically converged average configuration for solvent effects, *Chemical Physics Letters*, **437**, 148 (2007). DOI: 10.1016/j.cplett.2007.02.012.

[43] L. Lorenz, Ueber die Refractions constante, *Annalen der Physik*, **247**, 70 (1880). DOI: 10.1002/andp.18802470905.

[44] H.A. Lorentz, Ueber die Beziehung zwischen der Fortpflanzungsgeschwindigkeit des Lichtes und der Körperdichte, *Annalen der Physik*, **245**, 641 (1880), DOI: 10.1002/andp.18802450406.

[45] D.A. Kleinman, Nonlinear Dielectric Polarization in Optical Media, *Phys. Rev.*, **126**, 977 (1962). DOI: 10.1103/PhysRev.126.1977.

[46] H.A. Kurtz, D.S. Dudis, Quantum Mechanical Methods for Predicting Nonlinear Optical Properties, Reviews in Computational Chemistry, John Wiley & Sons, Inc., (2007) 241–279. DOI: 10.1002/9780470125892.ch5.

[47] Plaquet, Aurélie and Guillaume, Maxime and Champagne, Benoît and Castet, Frédéric and Ducasse, Laurent and Pozzo, Jean-Luc and Rodriguez, Vincent, In silico optimization of merocyanine-spiropyran compounds as second-order nonlinear optical molecular switches, Phys. Chem. Chem. Phys. 10 (2008) 6223-6232. DOI: 10.1039/B806561F.

[48] Y. Zhao, D. G. Truhlar, The M06 suite of density functionals for main group thermochemistry, thermochemical kinetics, noncovalent interactions, excited states, and transition elements: two new functionals and systematic testing of four M06-class functionals and 12 other functionals, *Theor. Chem. Acc.*, **120**, 215 (2008). DOI: 10.1007/s00214-007-0310-x.

[49] A.D. McLean, G. S. Chandler, Contracted Gaussian-basis sets for molecular calculations. 1. 2nd row atoms, Z=11-18, *J. Chem. Phys.*, **72**, 5639 (1980). DOI: 10.1063/1.438980.

[50] K. Raghavachari, J.S. Binkley, R. Seeger, J.A. Pople, Self-Consistent Molecular Orbital Methods. 20. Basis set for correlated wave-functions, *J. Chem. Phys.*, **72**, 650 (1980). DOI: 10.1063/1.438955.

[51] M.J. Frisch, G.W. Trucks, H.B. Schlegel, G.E. Scuseria, M.A. Robb, J.R. Cheeseman, G. Scalmani, V. Barone, G.A. Petersson, H. Nakatsuji, X. Li, M. Caricato, A. Marenich, J. Bloino, B.G. Janesko, R. Gomperts, B. Mennucci, H.P. Hratchian, J.V. Ortiz, A.F. Izmaylov, J.L. Sonnenberg, D. Williams-Young, F. Ding, F. Lipparini, F. Egidi, J. Goings, B. Peng, A. Petrone, T. Henderson, D. Ranasinghe, V.G. Zakrzewski, J. Gao, N. Rega, G. Zheng, W. Liang, M. Hada, M. Ehara, K. Toyota, R. Fukuda, J. Hasegawa, M. Ishida, T. Nakajima, Y. Honda,

O. Kitao, H. Nakai, T. Vreven, K. Throssell, J.A. Montgomery, Jr., J.E. Peralta, F. Ogliaro, M. Bearpark, J.J. Heyd, E. Brothers, K.N. Kudin, V.N. Staroverov, T. Keith, R. Kobayashi, J. Normand, K. Raghavachari, A. Rendell, J.C. Burant, S.S. Iyengar, J. Tomasi, M. Cossi, J.M. Millam, M. Klene, C. Adamo, R. Cammi, J.W. Ochterski, R.L. Martin, K. Morokuma, O. Farkas, J.B. Foresman, , D.J. Fox. Gaussian 09, Revision A.02 (2016). Gaussian Inc. Wallingford CT

[52] T. Lu, F. Chen, Multiwfn: A multifunctional wavefunction analyzer, *J. Comput. Chem.* **33**, 580 (2012). DOI: 10.1002/jcc.22885.

[53] V. Manzoni, L. Modesto-Costa, J. Del Nero, T. Andrade-Filho, R. Gester, Strong enhancement of NLO response of methyl orange dyes through solvent effects: A sequential Monte Carlo/DFT investigation, *Opt. Mat.* **94**, 152 (2019) DOI: 10.1016/j.optmat.2019.05.018.

[54] A. Raiol, A.R. da Cunha, V. Manzoni, T. Andrade-Filho, R. Gester, Solvent enhancement and isomeric effects on the NLO properties of a photoinduced cis-trans azomethine chromophore: A sequential MC/QM study, *J. Mol. Liq.* **340**, 116887 (2021). DOI: 10.1016/j.molliq.2021.116887.

[55] R.M. Gester, H.C. Georg, S. Canuto, M.C. Caputo, P.F. Provasi, NMR Chemical Shielding and Spin-Spin Coupling Constants of Liquid NH3: A Systematic Investigation using the Sequential QM/MM Method, *J. Phys. Chem. A.* **113** , 14936 (2009). DOI: 10.1021/jp9050484.

[56] R.M. Gester, C.Bistafa, H.C. Georg, K. Coutinho, S. Canuto, Theoretically describing the ^{17}O magnetic shielding constant of biomolecular systems: uracil and 5-fluorouracil in water environment, *Theor, Chem. Acc.* **133**, 1424 (2014). DOI: 10.1007/s00214-013-1424-y.

[57] R.M. Gester, H.C. Georg, T.L. Fonseca, P.F. Provasi, Sylvio Canuto, A simple analysis of the influence of the solvent-induced electronic polarization on the 15N magnetic shielding of pyridine in water, *Theor. Chem. Acc.* **131**, 1220 (2012) DOI: 10.1007/s00214-012-1220-0.

[58] R. Gester, M.V.A. Damasceno, S. Canuto, V. Manzoni, A theoretical study of the magnetic shielding of ^{15}N of formamide in liquid water, *J. Mol. Liq.* **320**, 114415 (2020). DOI: 10.1016/j.molliq.2020.114415.

[59] L. Modesto-Costa, R.M.Gester, V. Manzoni, The role of electrostatic interactions and solvent polarity on the ^{15}N NMR shielding of azines, *Chem. Phys. Lett.* **686**, 189 (2017). DOI: 10.1016/j.cplett.2017.08.031.

[60] T.S. Moss, Relations between the refractive index and energy gap of semiconductors, *Phys. Status Solidi B Basic Res.* **131**, 415 (1885). DOI: 10.1002/pssb.2221310202.

[61] Vinícius Manzoni, Rogerio Gester, Antonio R. da Cunha, Tarciso Andrade-Filho, Rodrigo Gester, Solvent effects on Stokes shifts, and NLO response of thieno[3,4-b] pyrazine: A comprehensive QM/MM investigation, Journal of Molecular Liquids 335 (2021) 115996. DOI: 10.1016/j.molliq.2021.115996.

[62] Marcos V. A. Damasceno, Vinícius Manzoni, Lucas Modesto-Costa, Geanso M. Moura, Jordan Del Nero, Alberto Torres, Rodrigo Gester, Solvent efects on low-lying absorptions and vibrational spectra of thieno[3,4-b]pyrazines: the role of unconventional C−H···N bonds, Chemical Papers, 73, 1519-1527 (2019). DOI: 10.1007/s11696-019-00703-2.

[63] J. L. Oudar and D. S. Chemla. Hyperpolarizabilities of the nitroanilines and their relations to the excited state dipole moment. The Journal of Chemical Physics, 66(6):2664–2668, 1977. DOI: doi.org/10.1063/1.434213.

[64] N.M. Ravindra, P. Ganapathy, J. Choi, Energy gap-refractive index relations in semiconductors - An overview, *Infrared Physics & Technology*, **50**, 21 (2007). DOI: 10.1016/j.infrared.2006.04.001.

[65] R.R. Reddy, Y Nazeer Ahammed, Relation between energy gap and electronic polarizability of ternary chalcopyrites, *Infrared Phys. Technol.* **37**, 505 (1996). DOI: 10.1016/1350-4495(95)00073-9.

[66] M.J. Alam, A.U. Khan, M. Alam, S. Ahmad, Spectroscopic (FTIR, FT-raman, 1H NMR and UV–vis) and DFT/TD-DFT studies on cholesteno [4,6-b,c]-20,50-dihydro-10,50-benzothiazepine, J. Mol. Struct. 1178 (2019) 570–582. DOI: 10.1016/j.molstruc.2018.10.063.

[67] H. Abbas, M. Shkir, S. AlFaify, Density functional study of spectroscopy, electronic structure, linear and nonlinear optical properties of l-proline lithium chloride and l-proline lithium bromide monohydrate: For laser applications, Arab. J. Chem. 12 (8) (2019) 2336–2346. DOI: 10.1016/j.arabjc.2015.02.011.

[68] K. Wu, J.G. Snijders, C. Lin, Reinvestigation of hydrogen bond effects on the polarizability and hyperpolarizability of urea molecular clusters, J. Phys. Chem. B 106 (35) (2002) 8954–8958. DOI: 10.1021/jp014181i.

Journal Pre-proof

Highlights

- Broad ultraviolet absorption band signalizing possible UV filter use.
- Intense and uncommon octupolar ($\beta_{J=3}$) feature.
- The solvent enhances the NLO response and improves the dipolar ($\beta_{J=1}$) characteristics.
- A possible dipolar/octupolar switch.

Declaration of competing interest

The authors declare that they have no known competing financial interests or personal relationships that could have appeared to influence the work reported in this paper.